

# COMPUTER SIMULATION OF QUANTUM SYSTEMS WITH FRICTION AND FEEDBACK

Andrey L. Sanin<sup>\*</sup>, Alexander A. Smirnovsky

Department of Theoretical Physics,

St. Petersburg State Polytechnical University, Polytekhnicheskaya 29, 195251, St. Petersburg, Russia

<sup>\*</sup>e-mail: andreylsanin@yandex.ru

**Abstract.** Dynamics of wave packets in quantum systems subjected to a friction force and impulse feedback is investigated in context of Schrödinger-Langevin-Kostin (SchLK) equation. The quantum systems with a quadratic potential bounded by impenetrable walls of a well are presented as examples. Numerical simulations are carried out for initial Gaussian packet at varied values of a friction coefficient and amplitudes of the impulse feedback. Informative and structural properties of the wave packets are analyzed by using Fourier transform of dynamical variables and their means, of autocorrelation Nauenberg's function. Coherent oscillations of the wave packets and transition to chaotic dynamics are found. Influence of friction on oscillatory dynamics is discussed.

## 1. Introduction

The quantum wave dynamics is of great theoretical and practical interest. Fundamental knowledge in this area is necessary for further development of quantum theory, informatics, and elaboration of single particle devices. If dissipative effects due to a macroscopic environment are weak, a quantum system can be considered as being isolated from the environment and can be described by using the Schrödinger equation or quantum hydrodynamic equations [1]. But the realization of isolated quantum systems in modern technologies is not simple and complete. One of obstacles for technical realization of a quantum computer is incoherence caused by coupling with environment and dissipative effects [2]. If the dissipative effects play an essential role, they must be accounted. Quantum dynamical equations involving dissipation, which are convenient for applications, present a challenging problem. In our paper we used the Schrödinger-Langevin-Kostin (SchLK) equation [3] that is often discussed in scientific literature [4, 5]. In this equation the dissipative term describes the "fluid" friction. The purpose of our investigation is to study the influence of friction on quantum system famous as "oscillator in box" [6-8]. In addition, we introduce a feedback model which is analogous to a model of classic watches. Detailed investigation of wave packet evolution is also a useful task of quantum informatics.

## 2. Basic equations and assumptions

The SchLK equation for the wave function  $\psi$  written in oscillatory units is

$$i \frac{\partial \psi}{\partial \alpha} = -\frac{1}{2} \frac{\partial^2 \psi}{\partial \alpha^2} + U_{\alpha} \psi + \frac{ik}{2} \left( \ln \frac{\psi}{\psi^*} - \left\langle \ln \frac{\psi}{\psi^*} \right\rangle \right) \psi, \quad (1)$$

where dimensionless quantities are used. Here  $\zeta$  and  $\tau$  are the position and time, respectively;

$U_{\Sigma} = U + U_{ext}$ , where  $U$  and  $U_{ext}$  are the static potential and the impulse potential, respectively;  $k$  is the friction coefficient. The symbol  $\langle \rangle$  denotes the mean value

$$\left\langle \ln \frac{\psi}{\psi^*} \right\rangle = \int \psi^* \ln \frac{\psi}{\psi^*} \psi d\zeta. \quad (2)$$

The quantum system of interest is confined by impenetrable walls at the points  $\zeta = \pm \zeta_L$ , where  $\zeta_L$  is the well half-width. The boundary conditions on the walls and the initial conditions are specified as

$$\psi(\zeta_L, \tau) = 0, \psi(\zeta, \tau = 0) = \psi_0(\zeta). \quad (3)$$

For the quadratic potential, we used the expression

$$U(\zeta) = \frac{1}{2} \zeta^2. \quad (4)$$

The potential (4) is confined by the impenetrable walls. The external potential exhibits the impulse force potential

$$U_{ext}(\zeta, \tau) = \begin{cases} F_0 \zeta, & \tau \in (\tau_s, \tau_s + \Delta\tau), \\ 0, & \tau \in (\tau_s, \tau_s + \Delta\tau). \end{cases} \quad (5)$$

Here  $F_0$  is the classic force defined with equation (5);  $\Delta\tau$  is the action duration of the impulse force. The time moments  $\tau_s$  in which the force is switched on can be defined by two ways. First is for the constrained force:  $\tau_s = nT$ , where  $T$  is the period of impulse repetition,  $n$  is an integer. Second is for feedback: in scientific literature it is well known as the theoretical model of a classic watch which includes the friction force and the force caused by potential (5), which switches on at defined times  $\tau_s$  when system is in some region of a phase space, for example, with  $\langle \zeta \rangle = 0$ ,  $\langle V \rangle \leq 0$ .

The quantity  $\ln \frac{\psi}{\psi^*}$  can be represented as

$$\ln \frac{\psi}{\psi^*} = i(2\arg(\psi) + 2n\pi), \quad (6)$$

where  $\arg(\psi) = \arctg\left(\frac{Im\psi}{Re\psi}\right)$  is the main phase value. In the above formulae,  $\psi^*$  is

the complex conjugate of the dimensionless wave function. It is necessary to note that physically correct solutions can be derived if the phase as a function of the position  $\zeta$  is continuous. In the calculations, we used the finite differences method with a second-order temporal and spatial approximation. The wave function normalization was controlled during the computation. Below, we also use the dimensionless quantities for the probability density  $N$  and the field velocity  $V$  defined as

$$N = \psi^* \psi, V = \frac{1}{2iN} \left( \psi^* \frac{\partial \psi}{\partial \zeta} - \psi \frac{\partial \psi^*}{\partial \zeta} \right). \quad (7)$$

The standard formulae for the mean values of the dynamic variables are

$$\langle \zeta \rangle = \int \psi^* \zeta \psi d\zeta, \quad \langle V \rangle = \int \psi^* \left( -i \frac{\partial}{\partial \zeta} \right) \psi d\zeta. \quad (8)$$

Here  $\langle \zeta \rangle$  is the mean position and  $\langle V \rangle$  is the mean velocity. To analyze the uncertainty relation, we also calculated the mean-quadratic variations of position and velocity in a standard quantum-mechanical manner. We designated these quantities as  $\langle (\Delta \zeta)^2 \rangle$ ,  $\langle (\Delta V)^2 \rangle$  and the standard deviations as  $\sigma_\zeta = \sqrt{\langle (\Delta \zeta)^2 \rangle}$ ,  $\sigma_V = \sqrt{\langle (\Delta V)^2 \rangle}$ . The product  $\sigma_\zeta \sigma_V$  is a function of time. Using the method of discrete Fourier transform described in Ref. [9], we analyzed only the modulus square  $|\Phi_{\langle \zeta \rangle}(\Omega)|^2$  as a function of  $\Omega$ ; here  $\Phi_{\langle \zeta \rangle}(\Omega)$  is the Fourier transform. Let us introduce the notation  $F_{\langle \zeta \rangle}(\Omega) = |\Phi_{\langle \zeta \rangle}(\Omega)|^2$ . Time evolution, revival structure of wave packets studied extensively in context of the autocorrelation function were introduced by Nauenberg and defined as

$$c(\tau) = \int_{\zeta_L}^{\zeta_L} (\zeta, \tau) \psi(\zeta, 0) d\zeta. \quad (9)$$

Its absolute square gives a measure of the overlap between the wave packet at times  $\tau = 0$  and  $\tau > 0$ . The quantity  $|c(\tau)|^2$  was applied for analysis of different quantum systems [10].

### 3. Driven oscillations of quantum wave packets

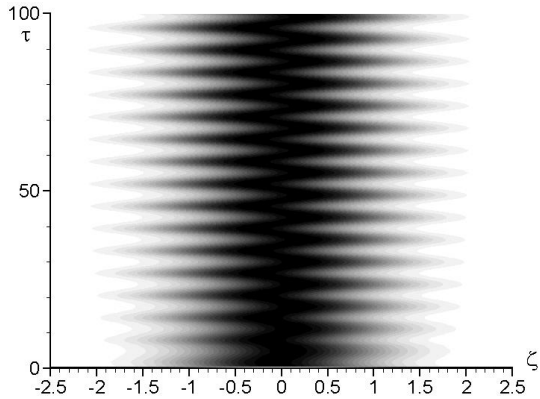
The simple dynamical regime takes place for the parameters  $F_0 = -0.5$ ,  $\Delta\tau = \pi / 16$ ,  $k = 0.1$ . The repetition period of impulse force is equal to  $2\pi$ . The initial Gaussian packet can be specified as

$$\psi_0(\zeta) = A \exp\left( \frac{1}{2} \zeta^2 + iV_0 \zeta \right), \quad (10)$$

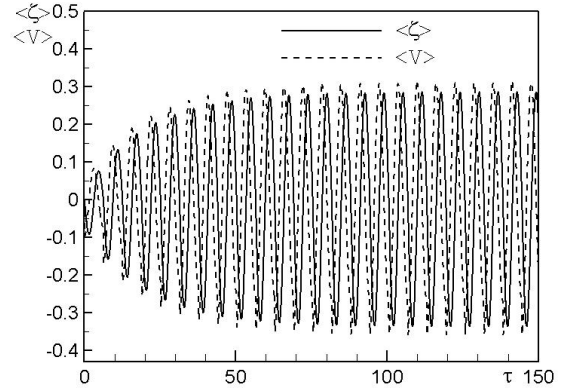
where  $A$  is defined from the normalization condition,  $-4 \leq \zeta \leq 4$ ,  $V_0 = 0$ . To analyze the dynamics of quantum wave packet, it is useful to construct the map of values for the probability density  $N$  in the plane  $(\zeta, \tau)$ . In three-dimensional space  $(\zeta, \tau, N)$  function  $N = N(\zeta, \tau)$  represents the surface, where  $N$  is height, and  $\zeta, \tau$  are coordinate in the plane  $(\zeta, \tau)$ . The planes  $N = \text{const}$  give lines, the projections of these lines on the plane  $(\zeta, \tau)$  form the map of values (levels)  $N$ . The calculations were performed in time interval  $[0, 300]$ . The dynamical properties are illustrated in Fig. 1.

In Fig. 1a we see the distribution of the probability density  $N$  including the width evolution of  $N$ ; the mean quantities  $\langle \zeta \rangle$ ,  $\langle V \rangle$  change in time is shown in Fig. 1b. After the transition region at  $\tau \in [0, 70]$ , the oscillations have a same amplitude. Accordingly one can see in Fig. 1c the main peak of function  $F_{\langle \zeta \rangle}(\Omega)$  which takes place at  $\Omega = 1$  (the frequency of impulse repetition). The high harmonics  $F_{\langle \zeta \rangle}(2)$ ,  $F_{\langle \zeta \rangle}(3)$ , ... are very weak. The product  $\sigma_\zeta \sigma_V$  has minimal value 0.5. Instead of analyzing the phase space  $(\langle \zeta \rangle, \langle V \rangle, \tau)$  we investigated the projections of phase trajectories in plane  $(\langle \zeta \rangle, \langle V \rangle)$ . For the sake of simplicity, let us introduce term "phase trajectories in plane  $(\langle \zeta \rangle, \langle V \rangle)$ ". This phase trajectory

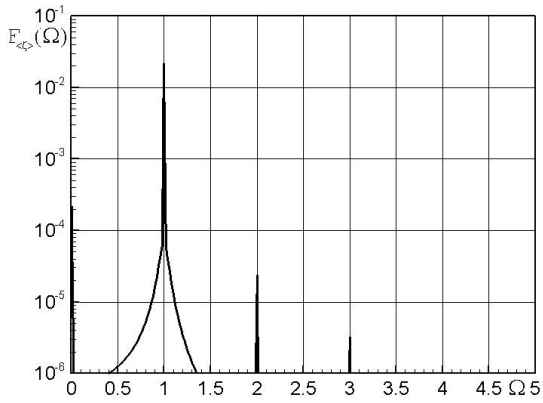
is presented in Fig.1d, it originates from the initial point ( $\langle \zeta \rangle = 0, \langle V \rangle = 0$ ) in a phase plane and will spiral to the following step and etc. Finally, the trajectory transforms to limiting one. The properties of limiting trajectory can be studied by help of stroboscope mapping and the function  $R_{n+1} = f(R_n)$  where  $R_n = \sqrt{\langle \zeta \rangle_n^2 + \langle V \rangle_n^2}$ . Index  $n$  corresponds to the discrete times  $\tau_n = nT, n = 0, 1, \dots, T = 2\pi$ . The numerical calculations are presented in Figs. 1e, f. We see that  $R_n$  tends to limiting point  $R_c$ . The quantity  $\left. \frac{df}{dR} \right|_{R_c} = \lim_{n \rightarrow \infty} \frac{R_{n+1} - R_n}{R_n - R_{n-1}}$  is equal 0.73. It means the existence of a stable attractor.



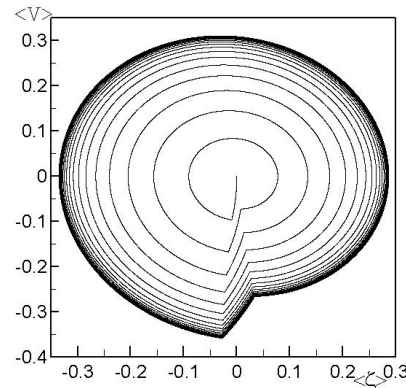
(a) Map of the probability density  $N$  in a plane ( $\zeta, \tau$ )



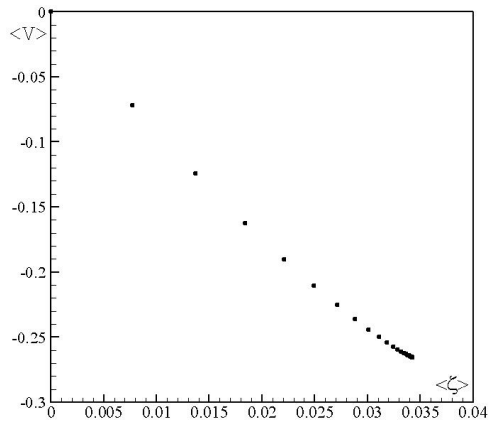
(b) Evolution of mean  $\langle \zeta \rangle, \langle V \rangle$



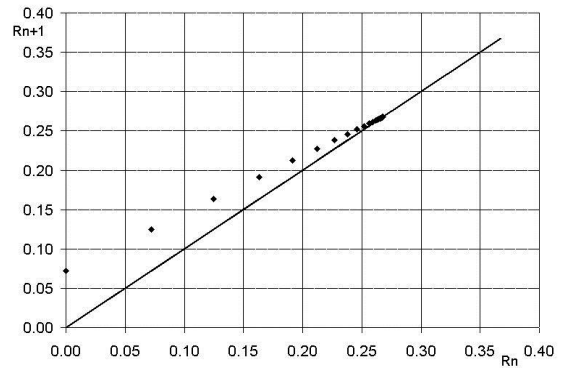
(c)  $F_{\langle \zeta \rangle}(\Omega)$  for  $\langle \zeta \rangle$



(d) Phase trajectories in a plane ( $\langle \zeta \rangle, \langle V \rangle$ )



(e) Stroboscope mapping



(f) Mapping  $R_{n+1} = f(R_n)$

**Fig. 1.** Driven oscillations.

#### 4. Quantum systems with impulse feedback

A non-stationary analysis was carried out for the initial Gaussian packet with  $\langle \zeta \rangle = 0$ ,  $\langle V \rangle = -1$ ,  $\sigma_\zeta \ll \zeta_L$ ; the other parameters are  $F_0 = -0.5$ ,  $k = 0.1$ ,  $\Delta\tau = \pi/16$ . The dynamical properties are illustrated in Fig. 2. The oscillations of probability density have the transition region  $\tau \in [0, 70]$  where the amplitude gradually reduces and then at  $\tau > 70$  becomes the same (Fig. 2a).

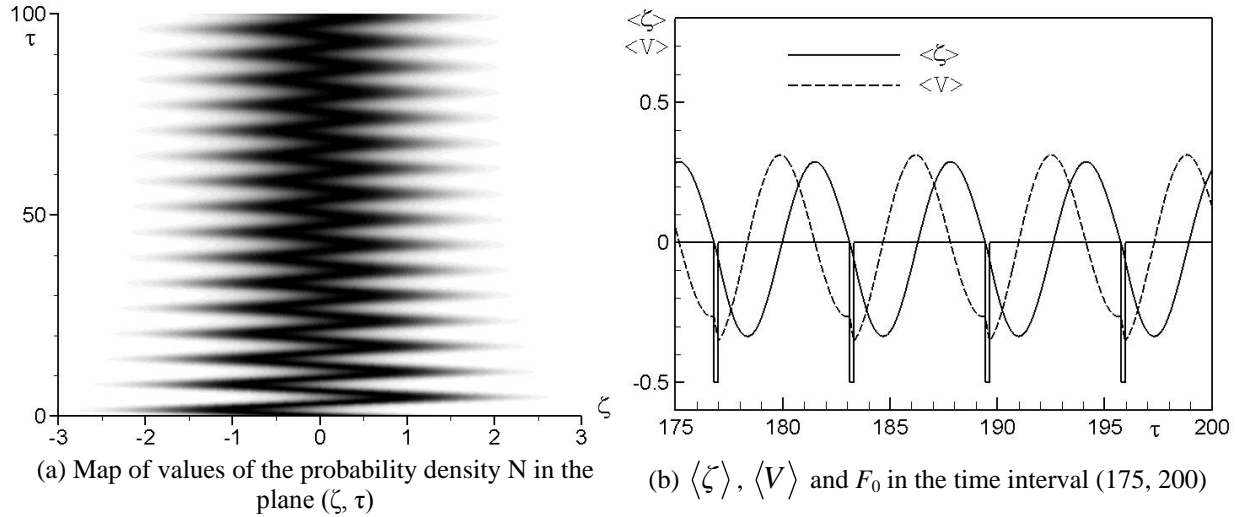


**Fig. 2.** Quantum analogy with a classic watch.

Parameters:  $F_0 = -0.5$ ,  $V_0 = -1$ ,  $k = 0.1$ .

Time realizations for the mean  $\langle \zeta \rangle$ ,  $\langle V \rangle$  are presented in Fig. 2b. Here, the sequential switches of  $F_0$  are taking place through the equal time spacing  $\Delta\tau_s = \tau_{s+1} - \tau_s$  between impulses. The classic scale  $\Delta\tau_s \approx 2\pi$  defines the oscillatory period which is closed to the period of a quantum oscillator with quadratic potential in the infinite rectangular well. The function  $F_{\langle \zeta \rangle}(\Omega)$  is characterized by the intensive peak at the frequency  $\Omega \approx 1$  ( $\Omega = 2\pi / \Delta\tau_s$ ), the higher harmonics are weak, for example,  $F_{\langle \zeta \rangle}(2) \approx 10^{-3} F_{\langle \zeta \rangle}(1)$ ,  $F_{\langle \zeta \rangle}(1) = 2 \cdot 10^{-2}$ . The calculations of Fourier-spectrum were fulfilled in the time interval  $[0, 200]$  including the transition region  $[0, 70]$ . For steady regime of oscillations, for example, at  $\tau \in [160, 200]$  the product  $\sigma_\zeta \sigma_V$  has a minimum 0.5. It is well known that a similar situation takes place for the coherent oscillations of the quantum harmonic oscillator in the whole interval  $(-\infty, \infty)$ . In this case the friction is not destructive. Furthermore, the oscillatory motion under dissipation and feedback for means  $\langle \zeta \rangle$ ,  $\langle V \rangle$  is likewise to one of a classic watch.

Varying the parameters  $F_0$  and  $k$ , other motion types were discovered and investigated in detail. The non-coherent regime of oscillations with discrete Fourier's spectrum is one of them. This type is identified by the high values  $\sigma_\zeta$ ,  $\sigma_V$ ; the product  $\sigma_\zeta \sigma_V$  is not minimal as for a harmonic oscillator; it can oscillate and change from 0.5 to large values. For example, the calculations performed for  $F_0 = -10$ ,  $V_0 = -1$  and  $k \in [0.167, 0.5]$  confirm the listed properties. However the Fourier spectrum is discrete for this type of oscillations. In the special case for the parameters  $F_0 = -10$ ,  $V_0 = -1$ ,  $k = 0.167$  the solutions of Eq. (1) are represented in Fig. 3. Now, the quantity  $\Delta\tau_s$  is not constant; in the average, it gradually decreases (Fig. 3a). In accordance with the  $\Delta\tau_s = f(\tau_s)$  for  $\tau_s > 200$ , the quantity  $\Delta\tau_s$  tends to the constant value  $\Delta\tau_s \approx 4.5$ , the corresponding frequency  $\Omega \approx 2\pi / \Delta\tau_s$  is equal to 1.395.

The probability density  $N(\zeta, \tau)$  is localized in the vicinity of well walls, in the center of system it is smeared out (Fig. 3b). The Fourier spectrum has a set of separate peaks (Fig. 3c), standard deviations  $\sigma_\zeta, \sigma_V$  are presented in Fig. 3d.

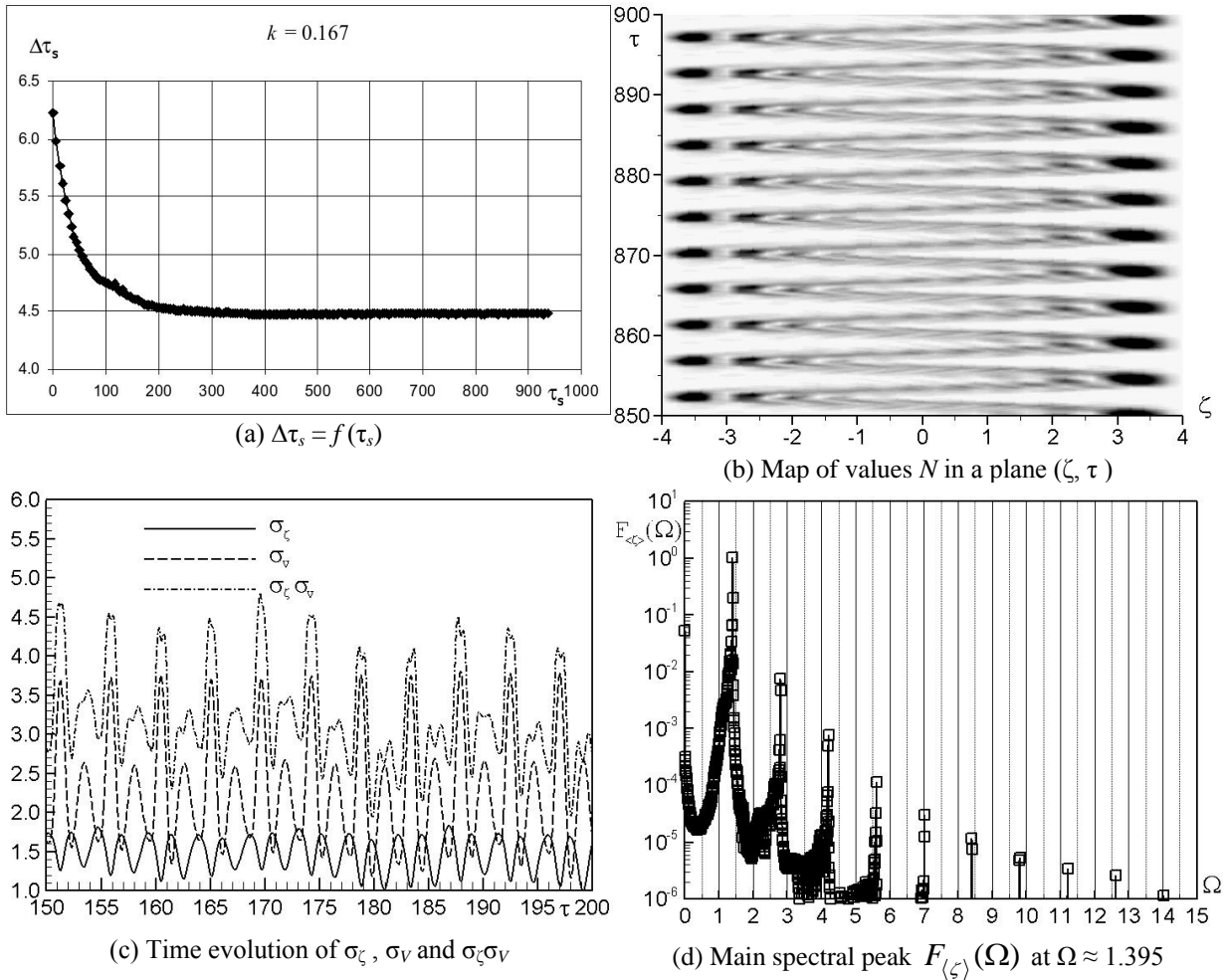


**Fig. 3.** Oscillations with non-minimal product  $\sigma_\zeta \sigma_V$  at  $k = 0.167$ .

If  $F_0 = -10$ ,  $V_0 = -1$  and  $k < 0.167$ , the more complex oscillatory motion is generated. It is characterized with dense Fourier's spectrum everywhere. The pair of values  $F_0 = -10$ ,  $k = 0.165$  can be considered as a bifurcation which defines the transition to chaotic oscillations. The structural properties of quantum wave packets are shown in Fig. 4. Now, the function  $\Delta\tau_s = f(\tau_s)$  consists of separate segments and quantum revivals (Fig. 4a). Here, we notice the time segments  $[0, 300]$ ,  $[325, 550]$ ,  $[590, 940]$  in which the function  $\Delta\tau_s = f(\tau_s)$  is a slowly dropping curve. In other shorter time segments, we see the rapid (non-monotonous) grow of  $\Delta\tau_s$  to maximal values. At time moments  $\tau_s$  the values  $\Delta\tau_s$  are nonuniform. The time realizations for  $\langle\zeta\rangle$ ,  $\langle V\rangle$  are presented in Fig. 4b. Structure of oscillations about  $\langle\zeta\rangle = 0$  is variable. These oscillations happen with the high product  $\sigma_\zeta \sigma_V$  (Fig. 4c). The spectral components  $F_{\langle\zeta\rangle}(\Omega)$  are presented at all frequencies  $\Omega \in [0, 20]$ ,  $\Omega = l \Omega_{min}$ ,  $l$  is an integer,  $\Omega_{min} = 2\pi/T$ ,  $T$  is the time interval of realization  $\langle\zeta\rangle$ . The values  $F_{\langle\zeta\rangle}(\Omega)$  for  $\Omega > 20$  become small and can be ignored. The calculations were performed for  $T = 1000, 2000, \dots$ . The calculations of the Nauenberg's autocorrelation function were also carried out, the results are shown in Fig. 4c. In comparison with the simple dynamic regimes represented in paper

[10], the picture of functional dependence  $|c(\tau)|^2$  becomes more complex. We see the overlap regions at  $\tau \approx 330, 580$  and the regions where  $|c(\tau)|^2$  is very small. The Fourier transform  $F_{|c(\tau)|^2}(\Omega)$  confirms the picture  $F_{\langle \zeta \rangle}(\Omega)$ , the spectrum being throughout dense too. The trajectory  $\langle V \rangle = f(\langle \zeta \rangle)$  in plane  $(\langle \zeta \rangle, \langle V \rangle)$  shows inhomogeneous distribution of phase points in the system (Fig. 4f).

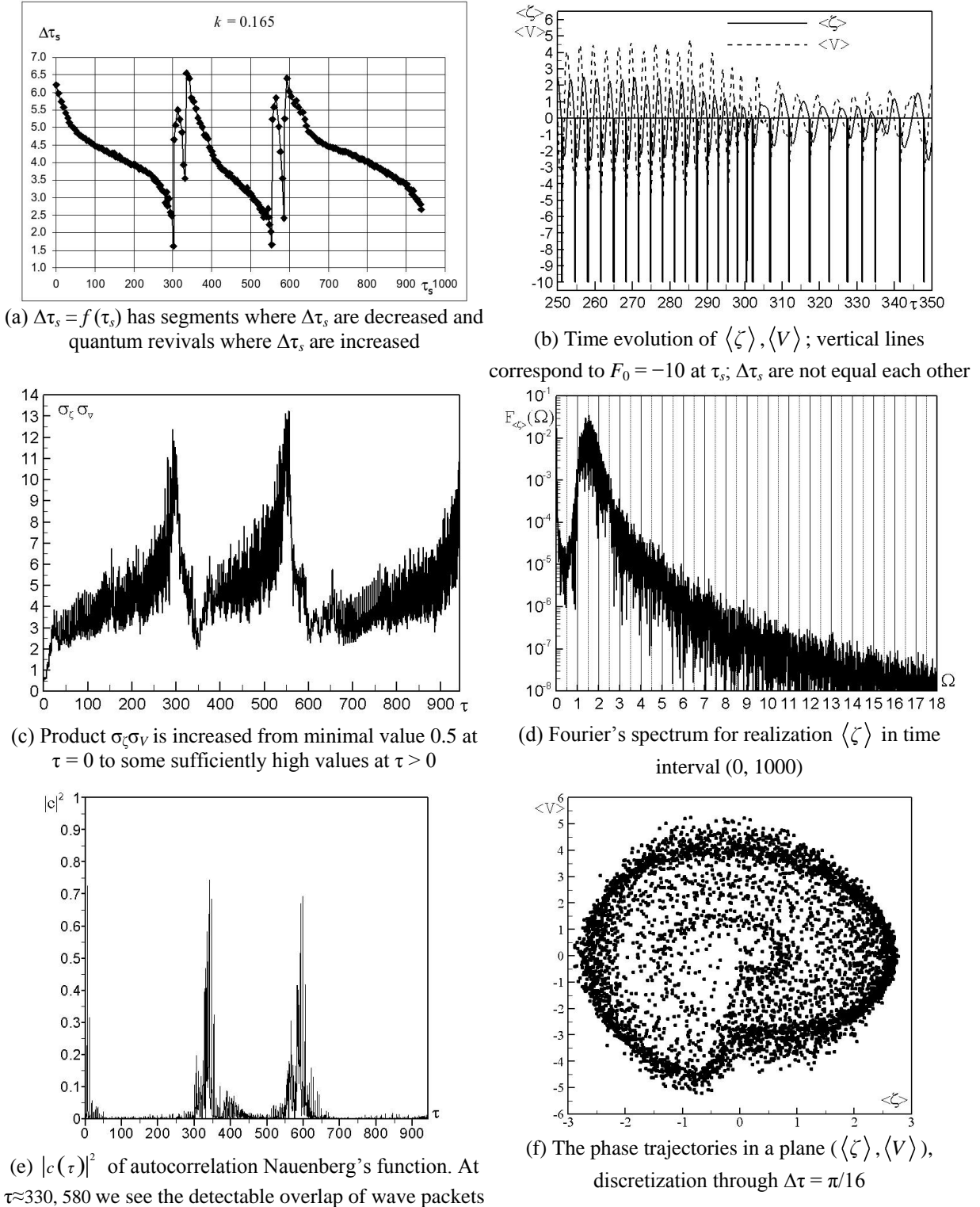


**Fig. 4.** Transition to complex oscillations at  $k = 0.165$ .

In addition, the investigations of  $V_{s+1}(V_s)$  were fulfilled. Here,  $V_s$  and  $V_{s+1}$  correspond to  $\langle V \rangle$  at times  $\tau_s$  and  $\tau_{s+1}$ , respectively. This dependence demonstrates the inhomogeneous distribution points in plane  $(V_s, V_{s+1})$ . If  $F_0 = -10$  and  $k$  is decreased to zero, the picture of oscillations remains chaotic. But, the properties of the chaotic oscillations are modified.

## References

- [1] P.R. Holland, *The Quantum Theory of Motion* (Cambridge University Press, Cambridge, 1993)
- [2] M.A. Nielsen, I.L. Chuang, *Quantum Computation and Quantum Information* (Cambridge University Press, Cambridge, 2000)
- [3] M.D. Kostin, M.D // *The Journal of Chemical Physics* **57** (1972) 3589.
- [4] H-D. Doebner, G.A. Goldin // *Physical Review A* **54** (1996) 3764.
- [5] A.L. Sanin, A.A. Smirnovsky // *Physics Letters A* **372** (2007) 21.
- [6] V.G. Gueorguiev, A.H.P. Rau, J.P. Draayer // *American Journal of Physics* **74** (2006) 394.
- [7] A.L. Sanin, A.A. Smirnovsky // *Proceedings of SPIE* **6597** (2007) 659704.
- [8] A.L. Sanin, A.A. Smirnovsky // *Izvestia VUZov: Prikladnaya Nelineinaya Dinamica (Proceedings of Higher Education: Applied Nonlinear Dynamics)* **15** (2007) 68.
- [9] J. Grindlay // *Canadian Journal of Physics* **79** (2001) 857.
- [10] R. Bluhm, V.A. Kosteletsky, J.A. Porter // *American Journal of Physics* **64** (1996) 944.